Modeling of formation and distribution of secondary aerosols in the Milan area (Italy)

S. Andreani-Aksoyoglu, A. S. H. Prévôt, U. Baltensperger, J. Keller, and J. Dommen
Laboratory of Atmospheric Chemistry, Paul Scherrer Institut, Villigen, Switzerland

Received 9 October 2003; revised 22 December 2003; accepted 12 January 2004; published 6 March 2004.

[1] The performance of an aerosol module of the three-dimensional Eulerian model CAMx (Comprehensive Air Quality Model with Extensions) was evaluated in a domain covering the Po Basin in northern Italy. Concentrations of secondary aerosol species such as particulate NO_3^-, NH_4^+, SO_4^{2-}, and SOC (secondary organic carbon) were calculated for the particle size below 2.5 μm and compared with the data available from a field experiment, which took place in May–June 1998. Model results for the inorganic aerosols were comparable to the measurements at an urban and a rural station. Sensitivity studies with reduced anthropogenic NO_x and volatile organic carbon (VOC) emissions showed that SOC behaves in the same way as ozone, i.e., decreases with reduced VOC emissions and increases with reduced NO_x emissions in the plume where ozone production is predicted to be VOC sensitive. Sensitivity of secondary aerosol formation to NH_3 and NO_x emissions was studied by reducing these emissions. Varying NH_3 emissions led to an almost linear change in secondary aerosol mass at sites with low NH_3. At ammonia-rich sites, on the other hand, availability of nitrate became important for the further formation of secondary aerosols. Monoterpene emissions were predicted to contribute about 25% of the secondary organic aerosols produced in the northern part of the model domain, which is mostly a forested area. *INDEX TERMS:* 0305 Atmospheric Composition and Structure: Aerosols and particles (0345, 4801); 0345 Atmospheric Composition and Structure: Pollution—urban and regional (0305); 0368 Atmospheric Composition and Structure: Troposphere—constituent transport and chemistry; *KEYWORDS:* aerosol modeling, CAMx, Po Basin, secondary aerosols, monoterpenes

Citation: Andreani-Aksoyoglu, S., A. S. H. Prévôt, U. Baltensperger, J. Keller, and J. Dommen (2004), Modeling of formation and distribution of secondary aerosols in the Milan area (Italy), *J. Geophys. Res.*, *109*, D05306, doi:10.1029/2003JD004231.

1. Introduction

[2] Aerosols play an important role in many environmental issues as climate change, acid rain, and smog. Although several studies were published on this subject in recent years [*Pandis et al.*, 1991, 1992; *Odum et al.*, 1996, 1997; *Mäkelä et al.*, 2000; *Griffin et al.*, 2002a], there still exists significant lack of knowledge in the relevant processes especially in the formation of secondary organic aerosols (SOA). Models that simulate the transport and transformation of aerosols and gases can contribute to improve the understanding of these processes. In recent years several air quality models have been upgraded to include aerosol dynamical processes such as coagulation, nucleation, evaporation, and condensation [*Ackermann et al.*, 1998; *Nenes et al.*, 1998; *Schell et al.*, 2001; *Pun et al.*, 2002; *Griffin et al.*, 2002b, 2003; *Makar et al.*, 2003]. In this study, the three-dimensional Eulerian model CAMx (Comprehensive Air Quality Model with Extensions) [*Environ International Corporation*, 2002] was applied to a domain in northern Italy for the first time including aerosol chemistry. The main objective is to investigate the capability of the model to predict the formation and spatial and temporal distribution of secondary organic and inorganic aerosols as well as the sensitivity of aerosol formation to anthropogenic and biogenic emissions.

[3] The northern part of the Po Basin is one of the most densely populated and strongly industrialized areas in Europe. The PIPAPO experiment (Pianura Padana Produzione di Ozono) was designed to investigate the photooxidant production in the Milan metropolitan region of Italy in summer 1998, within the frame of the European Experiment on Transport and Transformation of Environmentally Relevant Trace Constituents in the Troposphere Over Europe (EUROTRAC-2) project Limitation of Oxidants Production (LOOP) [*Neftel et al.*, 2002]. During this project, photooxidant production and limitation of ozone formation during two intensive observation periods (IOP1: 11–14 May, IOP2: 1–10 June) were studied using numerous measurements and models. *Dommen et al.* [2002] characterized the photooxidant formation in the Milan area using the aircraft measurements and reported high ozone mixing ratios between 100 and close to 200 ppb in the Milan region. Their analysis indicates volatile organic carbon (VOC) sensitive ozone formation within and downwind of the metropolitan area of Milan. NO_x and VOC dependence of ozone production was studied by *Thielmann*

Copyright 2004 by the American Geophysical Union.
0148-0227/04/2003JD004231$09.00

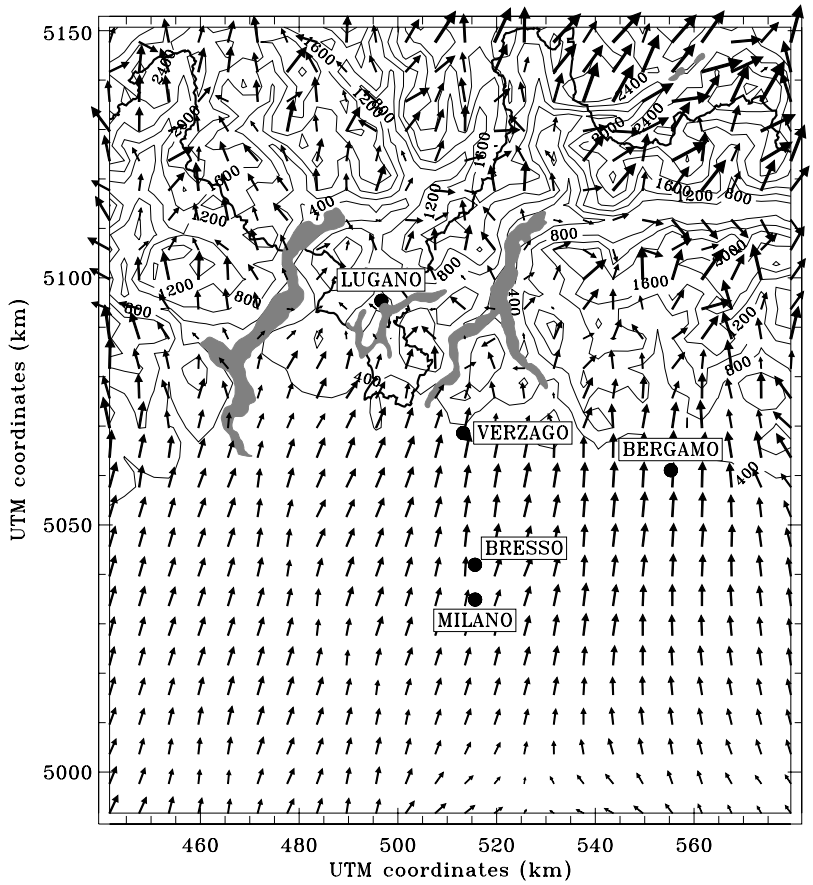

Figure 1. Modeled wind field in the lowest layer (0–50 m) on 13 May at 1500 central European standard time (CEST) shown over the topography (m asl).

et al. [2002] on the basis of measurements. They concluded that ozone production within the Po Basin has a tendency to be NO_x sensitive and that VOC sensitive ozone production is only occurring within the Milan urban plume. *Putaud et al.* [2002] investigated particulate matter chemical composition using the aerosol measurements carried out during the field experiment. There are also studies to investigate the photooxidant formation by means of three-dimensional model simulations [*Dosio et al.*, 2002; *Baertsch-Ritter et al.*, 2003a, 2003b; *Martilli et al.*, 2002]. However, these modeling studies were mainly focused on the gas-phase chemistry.

2. Model Description

2.1. Gas Phase Chemistry

[4] There are five gas-phase mechanisms supported in CAMx (Version 3.10). These are four different Carbon Bond Mechanism (CBM)-IV mechanisms (one with reactive chlorine chemistry, two with different isoprene chemistry, one with the aerosol chemistry) and the State Air Pollution Research Center (SAPRC99) chemical mechanism. Photolysis rates are derived for each grid cell assuming clear sky conditions as a function of five parameters: solar zenith angle, altitude, total ozone column, surface albedo, and atmospheric turbidity. Since the photolysis rates are significantly affected by the presence of clouds, a cloud input file is required in case of cloudy conditions which was not the case during the studied period. Dry deposition of gases is based on the resistance model of *Wesely* [1989]. In this study, CBM-IV (mechanism 4) was used to invoke the aerosol chemistry. It includes condensable organic gas species and a second olefin species to account for the biogenic olefins. The gas-phase chemistry governs the transformation of SO_2 to sulfate via the homogeneous gas-phase reaction, the production of nitric acid, and the production of condensable organic carbon.

2.2. Aerosol Chemistry

[5] The CAMx aerosol chemistry routine is a hybrid of the linear aqueous sulfate chemistry and parameterized sulfate/nitrate/ammonium equilibrium. In this mechanism, gaseous sulfate, nitric acid, and condensable organic carbon species, which are formed in the gas-phase chemistry, are supplied to the aerosol routine. Aqueous conversion of SO_2 to sulfate is calculated on the basis of relative humidity and seasonality. The equilibrium between sulfate, nitrate, and ammonium is handled in two modes. In ammonia-lean conditions, it is assumed that sulfate preferentially and irreversibly consumes all available ammonia. On the other hand, in ammonia-rich conditions, the equilibrium balance is parameterized according to regressions based on the detailed Sectional Equilibrium Model (SEQUILIB) approach as a function of temperature and humidity [*Pilinis and Seinfeld*, 1987]. Surface deposition of particles occurs via diffusion, impaction, and/or gravitational settling. The

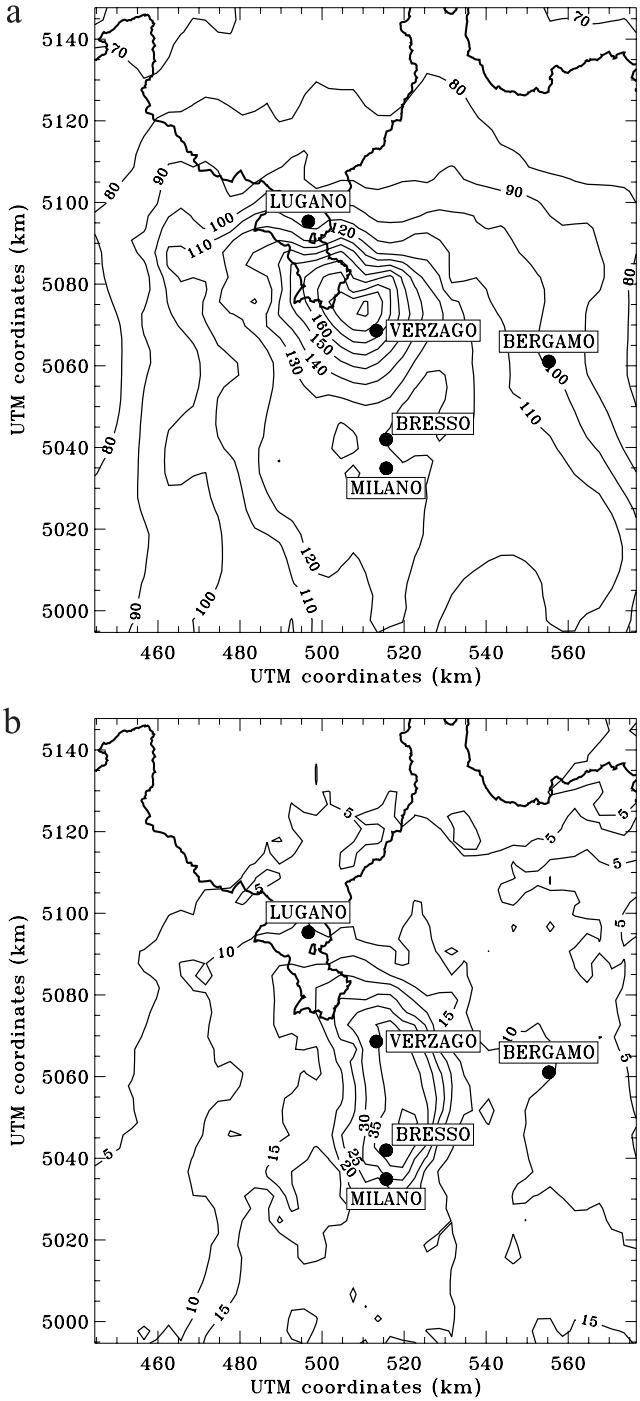

Figure 2. Predicted mixing ratios (ppb) of O_3 (a) and NO_y (b) on 13 May, 1500 CEST.

resistance approach used in Urban Airshed Model with Aerosols (UAM-AERO) [*Kumar et al.*, 1996] has been adopted in CAMx. The aerosol species calculated by CAMx include sulfate, nitrate, ammonium, organic carbon, sodium, chlorine, and primary inert PM (particulate matter). No particle size distribution is modeled in the version used, however the user can choose a representative size range and density for each aerosol species. In this study, the particle size range for the aerosol species was chosen as 0.04–2.5 μm, as indicated by experimental results [*Putaud et al.*, 2002].

2.3. Model Setup

[6] CAMx requires inputs to describe photochemical conditions, surface characteristics, initial and boundary conditions, emission rates, and various meteorological fields over the entire modeling domain. Details of the meteorological modeling using the SAI Mesoscale Model (SAIMM) are given elsewhere [*Baertsch-Ritter et al.*, 2003b]; therefore only a brief outcome of results will be given here. Meteorological simulations were performed for the period 9–13 May. The model was run with 19 layers. The modeled wind field on 13 May at 1500 central European standard time (CEST) is shown in Figure 1. The prevailing southerly wind during the day transports polluted air from Milan to the Alpine foothills in the north. The predicted surface wind speed of 2–3 m/s in the Po Basin is in agreement with observations. Hourly gridded vertical exchange coefficients were also calculated by the meteorological model to be supplied to CAMx. Other meteorological data supplied by the meteorological model are three-dimensional fields of temperature, pressure, and water vapor.

[7] Input data such as initial and boundary conditions and emissions were provided by the LOOP project community and are described elsewhere [*Baertsch-Ritter et al.*, 2003a]. An NH_3 emission inventory based on land use data was added to the LOOP emission inventory [*Martilli et al.*, 2002]. The model domain consists of 47 grid cells in the east-west direction and 54 grid cells in the north-south direction with a resolution of 3 km × 3 km. It covers the Lombardy region and some part of southern Switzerland (see Figure 1). There are eight layers in a terrain-following coordinate system, the first being 50 m above ground. The model top is set at 3000 m above ground. Simulations started on 11 May at 1200 central European summer time (CEST) and ended on 13 May at 2400 CEST. The first 12 hours were used to initialize the model; therefore only the results of 12 and 13 May will be discussed in this paper.

3. Results

3.1. Gaseous Species

[8] Several simulations were carried out by adapting the model and input parameters to find the closest match of results and observations before defining it as the base case. First simulations yielded too high SO_2 concentrations, which could be caused either by boundary conditions or emissions. Initial levels of SO_2 hardly influence the concentrations after 3 days of simulations; therefore they were not considered. The following sensitivity tests were performed: Ground level SO_2 emissions were reduced by a factor of 5, point source SO_2 emissions were removed, and boundary SO_2 concentrations were reduced by half. Effects of point sources and boundary concentrations were very small. After reducing the SO_2 ground level emissions, the predicted SO_2 concentrations were closer to the measurements. Therefore the case with reduced SO_2 emissions by a factor of 5 was defined as the base case for the following sections. Another modeling study using the same emission inventory also predicted too high SO_2 concentrations suggesting that emissions were probably overestimated

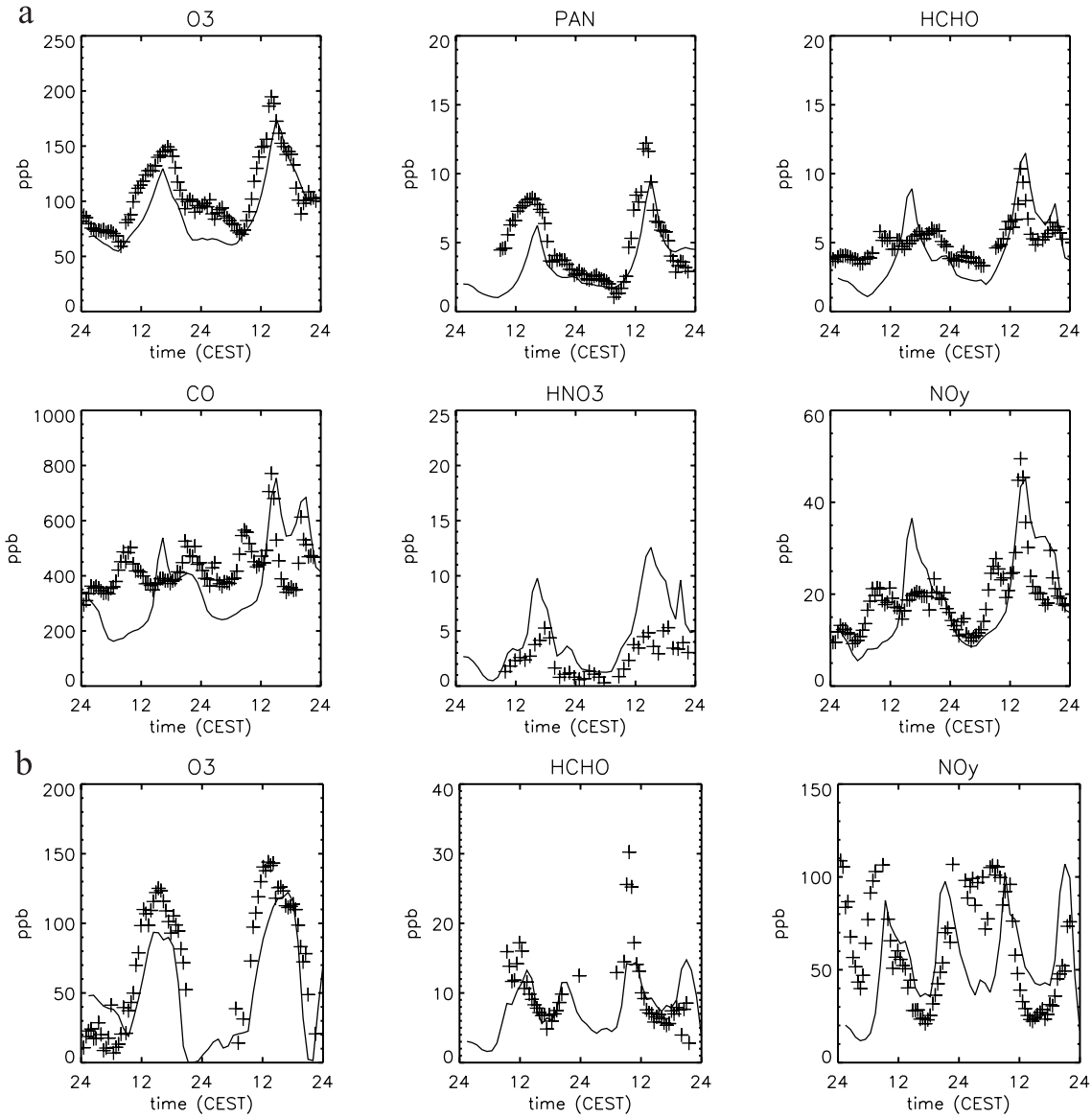

Figure 3. Diurnal variation of measured (plus symbol) and predicted (solid line) mixing ratios (ppb) for gaseous species during 12–13 May in (a) Verzago and (b) Bresso.

[*Martilli et al.*, 2002]. Emissions were referred to years 1991 and 1994 depending on the sources. Emissions for the year 1997 given by *Caserini et al.* [2001] are much lower than those used in the emission inventory. Therefore recently updated emission inventories are needed for future studies.

[9] Observations indicated that the photochemically active plume formed near Milan moved to the north. The ozone-mixing ratio reached about 195 ppb on 13 May at 1500 CEST near Verzago, which is about 30 km north of Milan. The predicted mixing ratios of O_3 and NO_y in the lowest model layer (layer top at 50 m) on 13 May at the time of peak ozone (1500 CEST) are shown in Figure 2. Highest ozone concentrations are predicted northwest of Verzago. Highest NO_y mixing ratios are found downwind of Milano. Figures 3a and 3b show the comparison of model results with ground-level measurements during 12–13 May in Verzago (semirural) and Bresso (urban), respectively. The diurnal cycles of ozone are well reproduced by the model at both sites. The predicted ozone peak on 13 May is delayed by about 1 hour in Verzago with respect to the observations. In the urban site Bresso, peak ozone is underestimated by about 20%. The predicted nighttime ozone concentrations are in good agreement with measurements at both sites. Model predictions for other species such as PAN, HCHO, CO, and NO_y are also satisfactory. The difference between the measured and calculated HNO_3 mixing ratios in the afternoon might be due to the underestimation in the measurements because HNO_3 measurements are known to be easily affected by losses in inlet lines. Low concentrations predicted at night match the measurements better.

3.2. Aerosol Species

3.2.1. Inorganic Aerosols

[10] Predicted levels of inorganic aerosols such as particulate NO_3^-, NH_4^+, and SO_4^{2-} in the model domain are shown

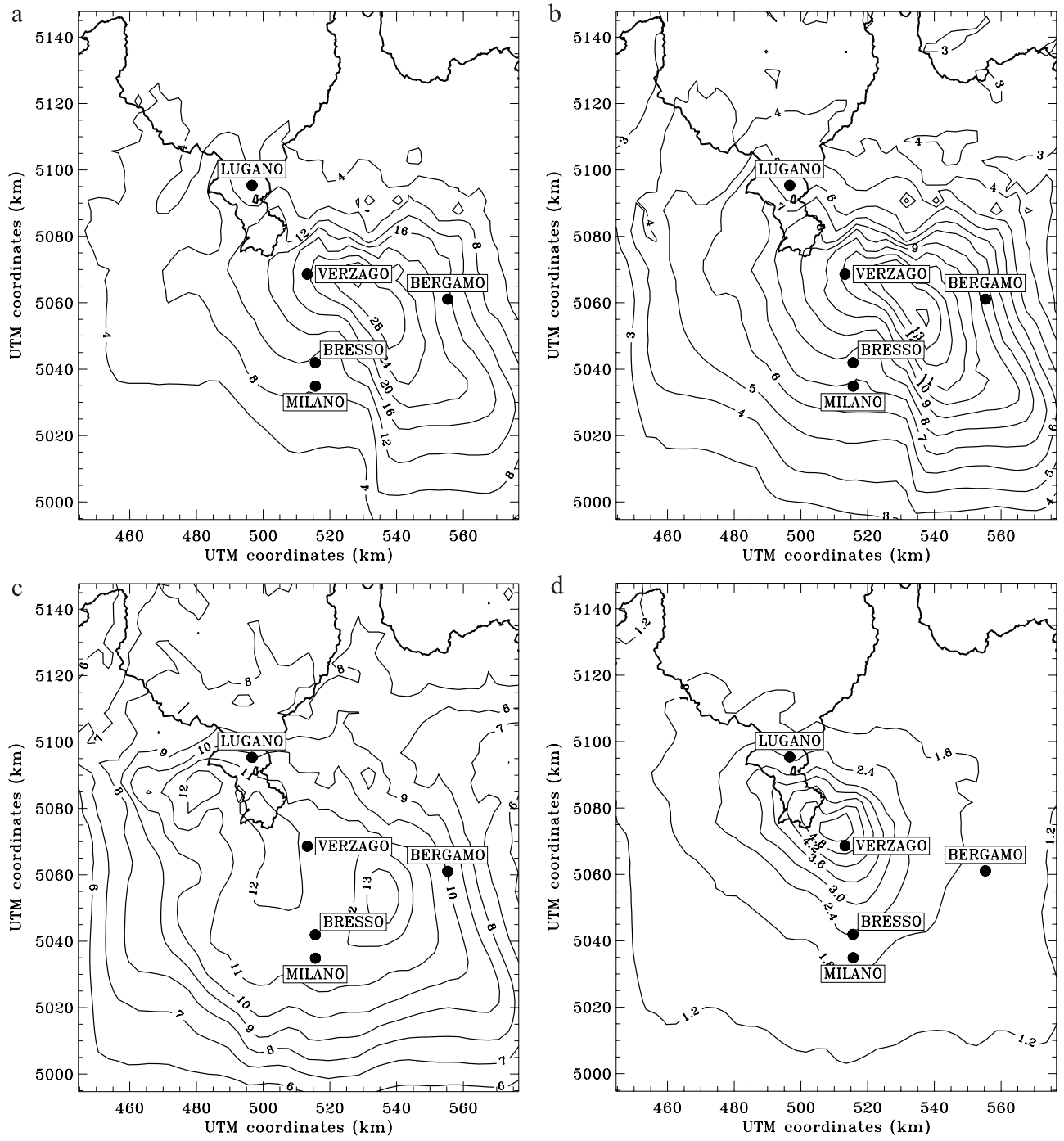

Figure 4. Predicted concentrations ($\mu g/m^3$) of particulate (a) NO_3^-, (b) NH_4^+, (c) SO_4^{2-}, and (d) secondary organic carbon (SOC) on 13 May, 1500 CEST.

in Figure 4. Particulate NO_3^- formation is driven by the NH_3 emissions, which are highest in the southeast corner of the domain. NO_3^- and NH_4^+ distributions are therefore similar. On the other hand, SO_4^{2-} concentrations are affected by SO_2 emissions. Inorganic aerosol components were measured online during 12–13 May in Verzago [*Baltensperger et al.*, 2002] and are shown in Figure 5a together with the model predictions. In Bresso, measurements during the period of interest are also available except for NH_4^+ (Figure 5b). The predicted particulate nitrate concentrations are close to the measurements especially on 13 May in both urban and semirural sites. Calculated sulfate and ammonium concentrations are also comparable to observations. The correlations between measured NH_4^+ and $NO_3^- + 2SO_4^{2-}$ at the urban site suggest that enough NH_3 was available to produce particulate NH_4NO_3 and $(NH_4)_2SO_4$ [*Putaud et al.*, 2002].

[11] *Baltensperger et al.* [2002] showed that the measured maximum nitrate/sulfate ratios occur at 1100 and 1530 CEST in Bresso and Verzago, respectively, indicating

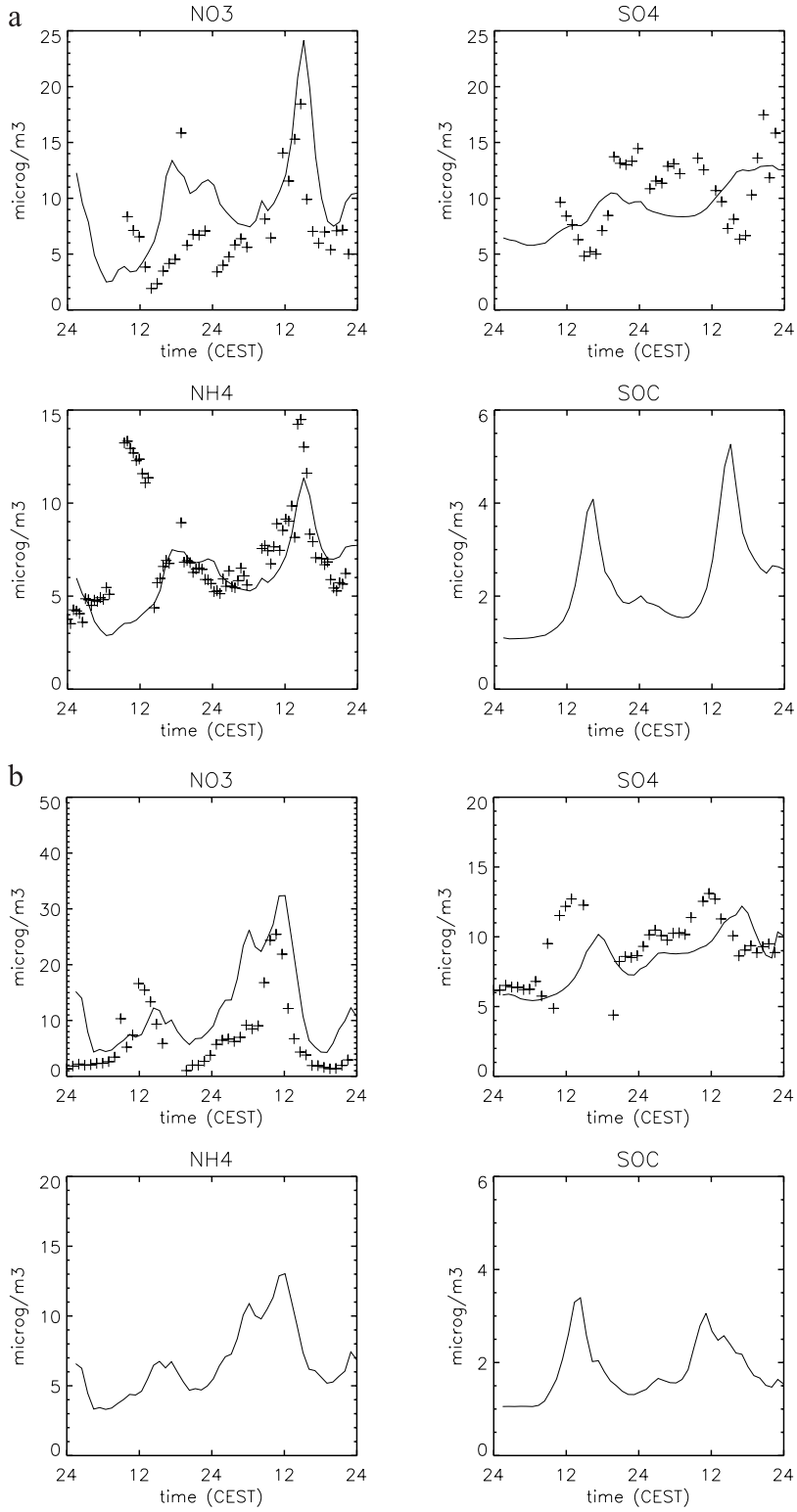

Figure 5. Diurnal variation of measured (plus symbol) and predicted (solid line) concentrations ($\mu g/m^3$) of particulate NO_3^-, SO_4^{2-}, NH_4^+, and SOC during 12–13 May in (a) Verzago and (b) Bresso.

that nitrate was formed during morning hours over Milan. The peak nitrate/sulfate ratio in Verzago coincides with the highest O_3 mixing ratio, suggesting the arrival of the Milan plume in the afternoon. Diurnal variations of nitrate/sulfate mixing ratios predicted by CAMx in Bresso and Verzago are shown in Figure 6. The model reproduced the same feature of a delayed peak of the nitrate/sulfate ratio in Verzago, which occurs at the same time of maximum ozone mixing ratio.

3.2.2. Organic Aerosols

[12] Organic aerosols contain both primary and secondary organic aerosols. Primary organic aerosols are not included

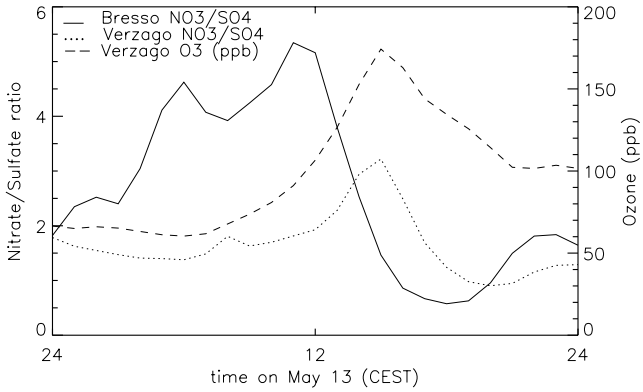

Figure 6. Diurnal variation of the predicted hourly nitrate/sulfate ratio in Bresso and Verzago on 13 May. The peak of the nitrate/sulfate ratio in Verzago is delayed compared with Bresso and coincides with the highest ozone-mixing ratio at this site.

in this study due to the lack of emission data. The predicted SOC concentrations are shown in Figure 4d. The highest levels are predicted in the afternoon near Verzago as in the case of ozone. Secondary organic aerosols are formed in the atmosphere by the mass transfer to the aerosol phase of low vapor pressure products of VOC oxidation. Therefore similar distribution in the domain as ozone can be expected. It is rather difficult to validate these results because of the following: There were only few measurements of total organic carbon (TOC) and black carbon (BC) in Bresso and Verzago. The measured TOC may contain both primary (POC) and secondary (SOC) organic carbon while model results refer only to SOC due to lack of emission data. Therefore a direct comparison of modeled SOC results with measured TOC concentrations cannot be done.

[13] BC, which is produced only in combustion processes and is therefore solely primary, can be used as a tracer of POC assuming that BC and POC have the same sources and that there is a constant ratio of POC/BC for the primary aerosol. Figure 7 shows the relationship between the TOC and BC concentrations measured in Bresso during the field experiment. The minimum value of TOC/BC ratio may be used as the ratio of primary organic aerosol to BC and is around 1.1 for urban areas [*Castro et al.*, 1999; *Viidanoja et al.*, 2002]. However, the ratio derived from Figure 7 is slightly higher (1.8). Using both ratios (1.8 derived from Figure 7, 1.1 reported in the literature) and the measured TOC and BC concentrations, amounts of SOC at both sites were estimated (Table 1). TOC and BC measurements were performed during various periods in May and June and therefore do not refer exactly to the same period as the simulations. The average SOC estimated using both ratios are in the same range as the values predicted by CAMx at both sites (Figures 5a–5b). Concentrations in Verzago are higher and the maximum levels are reached later than in Bresso. Considering the high uncertainties (about 50%) in the measurements [*Putaud et al.*, 2002] and in the estimation of the primary fraction of measured TOC and unknown uncertainties in the biogenic emissions, which play an important role in the SOC formation, the agreement between the measured and predicted values can be considered as satisfactory. The total secondary molar aerosol concentration (i.e., the sum of NO_3^-, SO_4^{2-}, NH_4^+, SOC) is highly correlated with secondary pollutants such as ozone ($r^2 = 0.87$) and formaldehyde ($r^2 = 0.91$) in Verzago. Although formaldehyde can be both primary and secondary, it is mostly secondarily produced in photochemically aged air. At the urban site Bresso the correlations were significantly lower ($r^2 = 0.2$ and 0.4 for ozone and formaldehyde, respectively).

3.3. Comparisons With Other Studies

[14] Although there were a few modeling studies during the LOOP project [*Dosio et al.*, 2002; *Baertsch-Ritter et al.*, 2003a, 2003b; *Martilli et al.*, 2002], it is rather difficult to compare them with our results because none of them modeled both inorganic and organic aerosol formation. The only study to be compared is the Topographic Vorticity Mesoscale Model with chemical model LCC (TVM-LCC) model system, which included a simple aerosol module to calculate inorganic aerosols [*Martilli et al.*, 2002]. There is no significant difference between the model results in case of ozone on 13 May. However, there are large differences between the two model results for the other species. TVM-LCC overestimated nighttime NO_y concentrations by about a factor of 6. CAMx on the other hand underestimated NO_y levels in the morning by about 40–50%. Afternoon values predicted by both models were very close to the measurements. In Verzago, both models overestimated afternoon HNO_3 concentrations. Night levels predicted by the CAMx match the measurements very well, whereas TVM-LCC produced a very high morning peak (8 times higher than the measurements). TVM-LCC had also a problem with maximum PAN concentrations, which were twice as high as the measured values. CAMx on the other hand could reproduce the measurements quite well for this species. Both models predicted much higher SO_2 concentrations than observations indicating an overestimation of SO_2 emissions in the

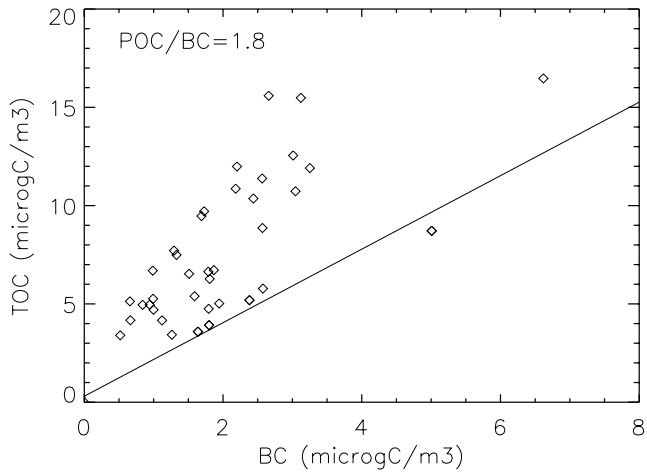

Figure 7. The relationship between black carbon and total organic carbon measured in Bresso. The minimum value of the total organic carbon (TOC)/black carbon (BC) ratio is assumed to represent the primary organic carbon (POC)/BC ratio.

Table 1. Estimation of Secondary Organic Carbon (SOC) From the Total Organic Carbon (TOC) and Black Carbon (BC) Measurements (TOC = POC + SOC), Using Two Different Primary Organic Carbon (POC)/BC Ratios (1.8 From Figure 7, 1.1 From *Castro et al.* [1999])[a]

Site	POC/BC	TOC ($\mu gC/m^3$)	BC ($\mu gC/m^3$)	POC ($\mu gC/m^3$)	SOC ($\mu gC/m^3$)
Bresso	1.8	6.5 ± 3.3	2.0 ± 1.2	3.6	2.9
	1.1			2.2	4.3
Verzago	1.8	5.6 ± 2.8	0.9 ± 0.6	1.6	4.0
	1.1			1.0	4.6

[a]TOC and BC values are the averages of about 40 samples measured during various periods in May and June 1998 [from *Putaud et al.*, 2002].

emission inventory. Concerning aerosol species, *Martilli et al.* [2002] discuss only the results of particulate NO_3^- and SO_4^{2-} in Verzago. TVM-LCC underestimated the afternoon nitrate levels by about 50% and overestimated nighttime and morning levels by 10 times. The performance of CAMx is significantly better. Model results for the morning match the measurements and afternoon values could be reproduced within 30%. Both models predicted increased SO_4 concentrations in the afternoon whereas measurements showed a decrease, which cannot be explained. CAMx reproduced particulate NH_4^+ on 13 May within 20%. No result was shown for this species in the work of *Martilli et al.* [2002].

3.4. Effects of Emission Reductions

3.4.1. NO_x and VOC Sensitivity

[15] Two simulations were performed with reduced NO_x and VOC emissions, each 35% separately. About 97% of NO_x is emitted as NO in the emission inventory [*Dommen et al.*, 2003], which was not changed in the sensitivity studies. Changes in predicted ozone concentrations due to the reductions of NO_x and VOC emissions are shown in Figure 8. Blue colors indicate the locations where ozone formation is VOC sensitive and red colors show the NO_x sensitive areas. Under the conditions studied, the plume is in the VOC sensitive regime as found also by *Baertsch-Ritter et al.* [2003a]. The next step is to see how the particulate species are affected by the reduction of ozone precursor emissions. Figure 9 shows the model results of particulate species as well as of ozone for the base case together with the perturbed emissions in Bresso and Lugano. In Bresso (Figure 9a), ozone production is mainly sensitive to VOC emissions, and therefore peak ozone concentrations decrease with VOC reductions while they increase with NO_x reductions. Secondary organic carbon aerosols show a similar behavior. SOC levels increase with NO_x reduction due to acceleration in the oxidation of VOCs to SOC. Particulate NH_4^+ and NO_3^- concentrations decrease with decreasing NO_x emissions because less nitric acid is produced. These species are not significantly affected by VOC

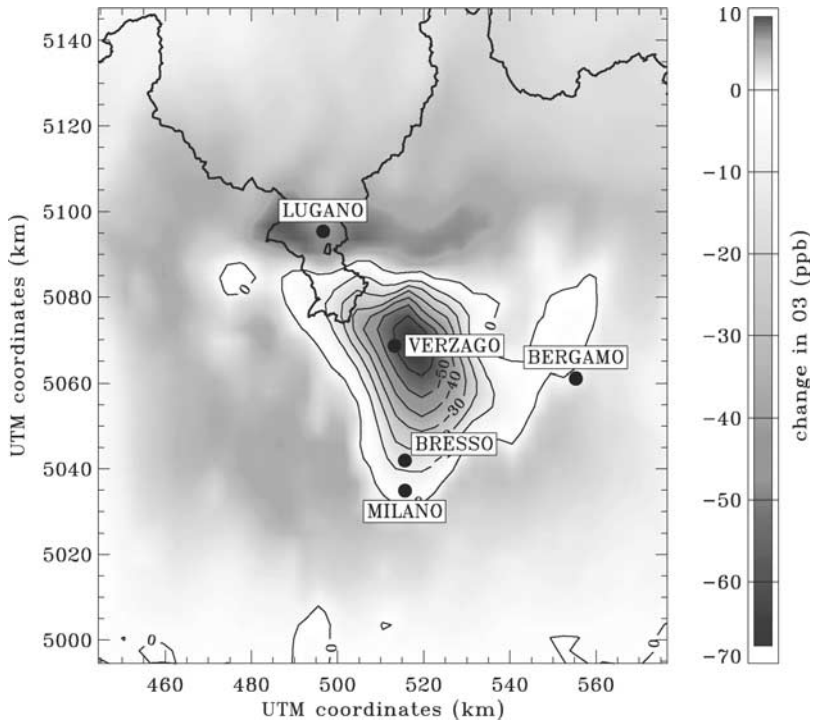

Figure 8. Changes in predicted O_3 mixing ratios (ppb) due to a 35% reduction of anthropogenic NO_x and VOC emissions on 13 May, 1500 CEST. Blue indicates volatile organic carbon (VOC) sensitive and red NO_x sensitive areas. See color version of this figure at back of this issue.

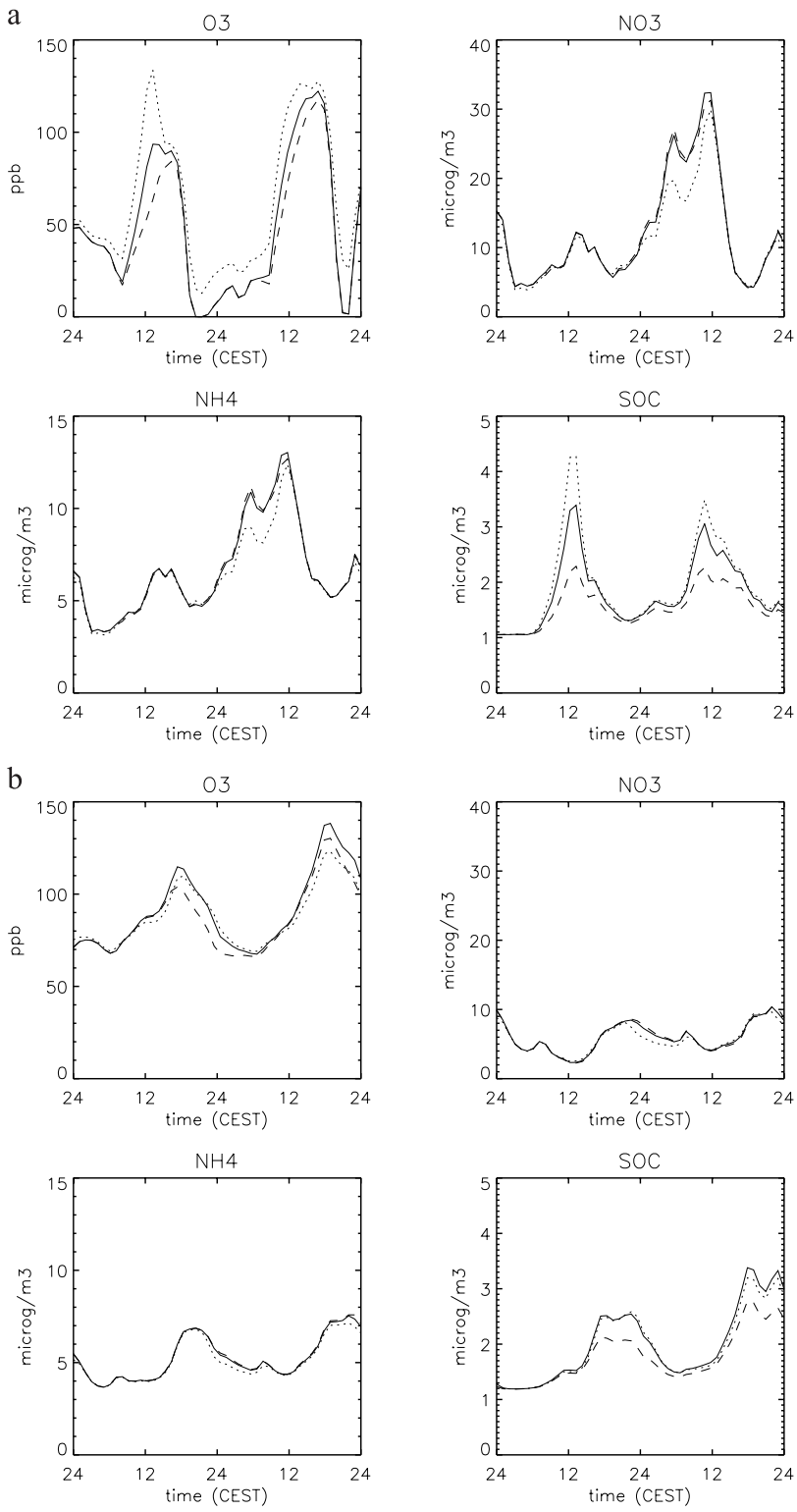

Figure 9. Ozone mixing ratios and concentrations of particulate NO_3^-, NH_4^+, and SOC for the base case (solid line) and for the cases with NO_x (dotted line) and VOC (dashed line) emission reductions in (a) Bresso and (b) Lugano.

emission reductions. In Lugano (Figure 9b), which is predicted to be in the NO_x sensitive regime, ozone concentrations decrease with both reduced precursor emissions. SOC levels decrease mainly due to VOC reductions and only slightly with NO_x reductions. Particulate NH_4^+ and NO_3^- levels are lower compared with those in Bresso and decrease slightly with reduced NO_x emissions.

3.4.2. NH_3 Sensitivity

[16] It was mentioned earlier that ammonia emissions used in the model have a large uncertainty. It is therefore

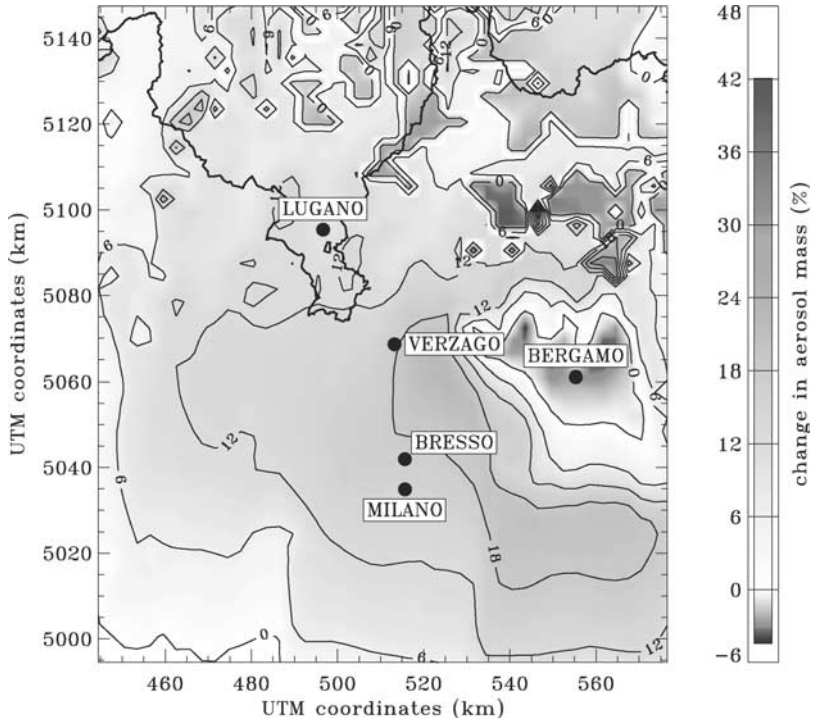

Figure 10. Changes in predicted secondary aerosol mass concentration (%) due to a 35% reduction of NO_x and NH_3 emissions on 13 May, 1500 CEST. Blue indicates NO_x sensitive and red indicates NH_3 sensitive areas. See color version of this figure at back of this issue.

important to know how the results can be affected by these emissions. Figure 10 shows the locations where secondary aerosol formation is sensitive to NH_3 and NO_x emissions. These results were derived from the model runs with reduced (35%) NH_3 and NO_x emissions. Blue colors indicate the areas where aerosol formation is more sensitive to NO_x emissions, whereas red regions are more NH_3 sensitive. In the base case, ammonia concentrations are highest in Bergamo. On the other hand, Verzago and Lugano represent the sites with the lowest ammonia levels. Secondary aerosol mass relative to the base case was plotted as a function of ammonia emissions relative to the base case for various sites (Figure 11). It is seen that aerosol mass increases almost linearly with increasing ammonia emissions at ammonia lean sites such as Verzago and Lugano, indicating NH_3 sensitivity of aerosol formation. On the other hand, in Bergamo, aerosol mass increases up to the level of the base case and then starts to level off. This indicates that no more nitrate is available to form NH_4NO_3 when NH_3 emissions are further increased.

3.5. Biogenic Versus Anthropogenic SOA

[17] With respect to the sources of precursor gases, secondary organic aerosols can be classified as anthropogenic and biogenic. Aromatics are the most significant anthropogenic SOA precursors [*Odum et al.*, 1997]. Biogenic hydrocarbons such as monoterpenes are among the most reactive gaseous compounds in the atmosphere, and they are important precursors of secondary organic aerosol [*Raes et al.*, 2000]. Discussion about the contribution of biogenic emissions to SOA formation became a very important topic in recent studies. Biogenic emissions were estimated to contribute around 15% of the SOA in urban areas with low vegetation like Los Angeles, while they are expected to dominate SOA in areas with high vegetation coverage like Atlanta [*Pandis et al.*, 1991, 1992]. Simulations carried out for an episode in July 1994 showed that biogenic SOA dominates compared with anthropogenic SOA over central Europe [*Schell et al.*, 2001]. *Andersson-Sköld and Simpson* [2001] showed that biogenic VOCs contribute far more to SOA formation in northern Europe than anthropogenic VOCs. Some studies showed that anthropogenic and biogenic SOA compounds may interact, and therefore increases in the production of one of them

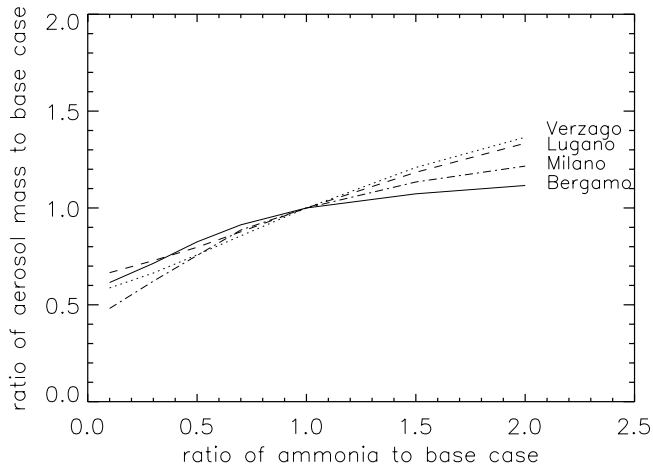

Figure 11. Change in aerosol mass due to a change in ammonia emissions relative to the base case on 13 May, 1500 CEST.

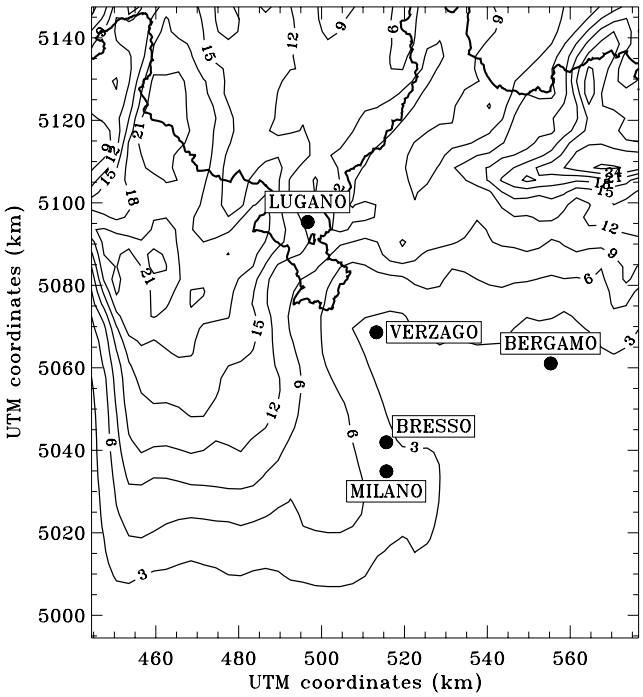

Figure 12. Contribution (%) of monoterpene emissions to SOC concentrations in the afternoon.

may lead to increases in the concentrations of the other by shifting their partitioning towards the particulate phase [*Kanakidou et al.*, 2000; *Schell et al.*, 2001]. In the region we studied, monoterpene emissions are highest in the forested areas at higher altitudes, which are in the northern part of the domain. Two simulations carried out with and without monoterpene emissions showed that monoterpenes contribute up to about 25% of the SOA produced on 13 May in this part (Figure 12). The contribution of biogenic emissions in the urban area of Milan is much less (3–6%). Some other European studies suggested a higher contribution of biogenic emissions to SOA formation [*Andersson-Sköld and Simpson*, 2001; *Schell et al.*, 2001]. The reasons of this discrepancy may be due to either biogenic emission inventories or their parameterization or treatment of aerosol formation in the models. In this study, there is no speciation of monoterpenes because CAMx treats biogenic olefins only with one species. The contribution of isoprene emissions was not investigated in this study because there has been no proven evidence so far about the SOA formation potential of isoprene oxidation products [*Seinfeld and Pandis*, 1998]. However, a recent study by *Matsunaga et al.* [2003] suggested that the concentrations of some oxidation products of isoprene in the particulate phase were comparable to that of oxidation products of monoterpenes. Their contribution should therefore be taken into account for the formation and growth of biogenic organic aerosols in future studies.

4. Conclusions

[18] The performance of an aerosol module of the three-dimensional Eulerian model CAMx was evaluated for the first time in a domain covering the Lombardy region in northern Italy. The secondary aerosol species such as particulate NO_3^-, NH_4^+, SO_4^{2-}, and SOC were calculated for the particle size below 2.5 μm and compared with the measurements available from the PIPAPO field experiment, which took place in May–June 1998. Concentrations of gaseous species could be reproduced by the model quite satisfactorily except for SO_2. Sensitivity tests indicated that SO_2 emissions were most probably overestimated. Model results for inorganic aerosols were comparable to the measurements both at urban and semirural stations. It was rather difficult to validate the model results of organic aerosols due to the lack of measurements. An indirect way of estimation of secondary organic aerosols from organic carbon and black carbon measurements showed that the predicted values were of the same order of magnitude. The total secondary particle mass concentration was highly correlated with secondary gaseous pollutants such as ozone and formaldehyde at the semirural site Verzago, in contrast to the urban site. In most of the model domain, particulate NO_3^- and NH_4^+ concentrations decreased with reduced NO_x emissions. On the other hand, the levels of secondary organic carbon aerosols decreased with reduced VOC emissions but increased with reduced NO_x emissions, similarly to ozone. Secondary aerosol mass was predicted to increase almost linearly with increasing ammonia emissions in the north where ammonia emissions are lowest and aerosol formation is NH_3 sensitive. Around Bergamo where ammonia levels are highest, formation of secondary aerosols was limited by the availability of nitric acid when emissions were further increased. Monoterpene emissions were predicted to contribute about 25% to the SOA production in the northern part of the model domain, which is mostly a forested area. In the southern part of the domain, which is mainly an urban and agricultural area, the contribution is negligible. In spite of the high uncertainties concerning NH_3 emissions and the simplicity of the aerosol module, model results can be considered as satisfactory. Improvement of emission data will be important to further improve the model results. To evaluate the model performance in more detail, more temporally and spatially resolved accurate measurements of the aerosol composition are needed.

[19] **Acknowledgments.** We would like to thank the LOOP community for providing us with various data and A. Martilli for providing the NH_3 emissions. Help of Chris Emery and Greg Yarwood from ENVIRON is gratefully acknowledged. This work is partly supported by the FORMAT (Formaldehyde as a tracer of photooxidation in the troposphere) project BBW 01.0233.

References

Ackermann, I. J., H. Hass, M. Memmesheimer, A. Ebel, F. S. Binkowski, and U. Shankar (1998), Modal aerosol dynamics model for Europe: Development and first applications, *Atmos. Environ.*, *32*, 2981–2999.

Andersson-Sköld, Y., and D. Simpson (2001), Secondary organic aerosol formation in Northern Europe: A model study, *J. Geophys. Res.*, *106*, 7357–7374.

Baertsch-Ritter, N., A. S. H. Prévôt, J. Dommen, S. Andreani-Aksoyoglu, and J. Keller (2003a), Model study with UAM-V in the Milan area (I) during PIPAPO: Simulations with changed emissions compared to ground and airborne measurements, *Atmos. Environ.*, *37*, 4143–4147.

Baertsch-Ritter, N., J. Keller, J. Dommen, and A. S. H. Prévôt (2003b), Effects of various meteorological conditions and spatial emission resolu-

tions on the ozone concentration and ROG/NO_x limitation in the Milan area (I), *Atmos. Chem. Phys. Discuss.*, *3*, 733–768.

Baltensperger, U., et al. (2002), Urban and rural aerosol characterization of summer smog events during the PIPAPO field campaign in Milan, Italy, *J. Geophys. Res.*, *107*(D22), 8193, doi:10.1029/2001JD001292.

Caserini, S., A. Fraccaroli, A. M. Monguzzi, M. Moretti, and A. B. Denti (2001), Lombardy region (Italy) emission inventory: Methodologies and results, paper presented at Emission Inventory Conference "One Atmosphere, One Inventory, Many Challenges," Environ. Prot. Agency, Denver, Colo.

Castro, L. M., C. A. Pio, R. M. Harrison, and D. J. T. Smith (1999), Carbonaceous aerosol in urban and rural European atmospheres: Estimation of secondary organic carbon concentrations, *Atmos. Environ.*, *33*, 2771–2781.

Dommen, J., A. S. H. Prévôt, B. Neininger, and M. Bäumle (2002), Characterization of the photooxidant formation in the metropolitan area of Milan from aircraft measurements, *J. Geophys. Res.*, *107*(D22), 8197, doi:10.1029/2000JD000283.

Dommen, J., A. S. H. Prévôt, N. Baertsch-Ritter, G. Maffeis, M. G. Longoni, F. C. Gruebler, and A. Thielmann (2003), High-resolution emission inventory of the Lombardy region: Development and comparison with measurements, *Atmos. Environ.*, *37*, 4149–4161.

Dosio, A., S. Galmarini, and G. Graziani (2002), Simulation of the circulation and related photochemical ozone dispersion in the Po plains (Northern Italy): Comparison with the observations of a measuring campaign, *J. Geophys. Res.*, *107*(D22), 8189, doi:10.1029/2000JD000046.

Environ International Corporation (2002), *Environ User's Guide: Comprehensive Air Quality Model With Extensions* (*CAMx*), version 3.10, Novato, Calif.

Griffin, R. J., D. Dabdub, and J. H. Seinfeld (2002a), Secondary organic aerosol: 1. Atmospheric chemical mechanism for production of molecular constituents, *J. Geophys. Res.*, *107*(D17), 4332, doi:10.1029/2001JD000541.

Griffin, R. J., D. Dabdub, M. J. Kleeman, M. P. Fraser, G. R. Cass, and J. H. Seinfeld (2002b), Secondary organic aerosol: 3. Urban/regional scale model of size- and composition resolved aerosols, *J. Geophys. Res.*, *107*(D17), 4334, doi:10.1029/2001JD000544.

Griffin, R. J., K. Nguyen, D. Dabdub, and J. H. Seinfeld (2003), A coupled hydrophobic-hydrophilic model for predicting secondary organic aerosol formation, *J. Atmos. Chem.*, *44*, 171–190.

Kanakidou, M., K. Tsigaridis, F. J. Denetener, and P. J. Crutzen (2000), Human-activity-enhanced formation of organic aerosols by biogenic hydrocarbon oxidation, *J. Geophys. Res.*, *105*, 9243–9254.

Kumar, N., F. W. Lurmann, A. S. Wexler, S. Pandis, and J. H. Seinfeld (1996), Development and application of a three dimensional aerosol model, paper presented at Specialty Conference on Computing in Environmental Resource Management, Air and Waste Manage. Assoc., Research Triangle Park, N. C.

Makar, P. A., et al. (2003), AURAMS runs during the Pacific2001 time period: A model/measurement comparison, paper presented at 26th International Technical Meeting on Air Pollution Modelling and its Application, North Atlantic Treaty Org., Brussels.

Mäkelä, J. M., M. D. Maso, L. Pirjola, P. Keronen, L. Laakso, M. Kulmala, and A. Laaksonen (2000), Characteristics of the atmospheric particle formation events observed at a boreal forest site in southern Finland, *Boreal Environ. Res.*, *5*, 299–313.

Martilli, A., A. Neftel, G. Favaro, F. Kirchner, S. Sillman, and A. Clappier (2002), Simulation of the ozone formation in the northern part of the Po Valley, *J. Geophys. Res.*, *107*(D22), 8195, doi:10.1029/2001JD000534.

Matsunaga, S., M. Mochida, and K. Kawamura (2003), Growth of organic aerosols by biogenic semi-volatile carbonyls in the forestall atmosphere, *Atmos. Environ.*, *37*, 2045–2050.

Neftel, A., C. Spirig, A. S. H. Prévôt, M. Furger, J. Stutz, B. Vogel, and J. Hjorth (2002), Sensitivity of photooxidant production in the Milan Basin: An overview of results from a EUROTRAC-2 Limitation of Oxidant Production field experiment, *J. Geophys. Res.*, *107*(D22), 8188, doi:10.1029/2001JD001263.

Nenes, A., S. N. Pandis, and C. Pilinis (1998), ISORROPIA: A new thermodynamic equilibrium model for multiphase multicomponent inorganic aerosols, *Aquat. Geochem.*, *4*, 123–152.

Odum, J. R., T. Hoffmann, F. Bowman, T. Collins, R. C. Flagan, and J. H. Seinfeld (1996), Gas-particle partitioning and secondary organic aerosol yields, *Environ. Sci. Technol.*, *30*, 2580–2585.

Odum, J. R., T. P. W. Jungkamp, R. J. Griffin, R. C. Flagan, and J. H. Seinfeld (1997), The atmospheric aerosol-forming potential of whole gasoline vapor, *Science*, *276*, 96–99.

Pandis, S. N., S. E. Paulson, J. H. Seinfeld, and R. C. Flagan (1991), Aerosol formation in the photooxidation of isoprene and β-pinene, *Atmos. Environ.*, *25A*, 997–1008.

Pandis, S. N., R. A. Harley, G. R. Cass, and J. H. Seinfeld (1992), Secondary organic aerosol formation and transport, *Atmos. Environ.*, *26A*, 2269–2282.

Pilinis, C., and J. H. Seinfeld (1987), Development and evaluation of an Eulerian photochemical gas-aerosol model, *Atmos. Environ.*, *21*, 2453–2466.

Pun, B. K., R. J. Griffin, C. Seigneur, and J. H. Seinfeld (2002), Secondary organic aerosol: 2. Thermodynamic model for gas/particle partitioning of molecular constituents, *J. Geophys. Res.*, *107*(D17), doi:10.1029/2001JD000542.

Putaud, J.-P., R. Van Dingenen, and F. Raes (2002), Submicron aerosol mass balance at urban and semirural sites in the Milan area (Italy), *J. Geophys. Res.*, *107*(D22), 8198, doi:10.1029/2000JD000111.

Raes, F., R. Van Dingenen, E. Vignati, J. Wilson, J.-P. Putaud, J. H. Seinfeld, and P. Adams (2000), Formation and cycling of aerosols in the global troposphere, *Atmos. Environ.*, *34*, 4215–4240.

Schell, B., I. J. Ackermann, H. Hass, F. S. Binkowski, and A. Ebel (2001), Modeling the formation of secondary organic aerosol within a comprehensive air quality modeling system, *J. Geophys. Res.*, *106*, 28,275–28,293.

Seinfeld, J. H., and S. Pandis (1998), *Atmospheric Chemistry and Physics, From Air Pollution to Climate Change*, John Wiley, Hoboken, N. J.

Thielmann, A., A. S. H. Prévôt, and J. Staehelin (2002), Sensitivity of ozone production derived from field measurements in the Italian Po basin, *J. Geophys. Res.*, *107*(D22), 8194, doi:10.1029/2000JD000119.

Viidanoja, J., M. Sillanpaa, J. Laakia, V.-M. Kerminen, R. Hillamo, P. Aarnio, and T. Koskentalo (2002), Organic and black carbon in PM2.5 and PM10: 1 year of data from an urban site in Helsinki, Finland, *Atmos. Environ.*, *36*, 3183–3193.

Wesely, M. L. (1989), Parameterization of surface resistances to gaseous dry deposition in regional-scale numerical models, *Atmos. Environ.*, *23*, 1293–1304.

S. Andreani-Aksoyoglu, U. Baltensperger, J. Dommen, J. Keller, and A. S. H. Prévôt, Laboratory of Atmospheric Chemistry, Paul Scherrer Institut, Villigen PSI, CH-5232, Switzerland. (sebnem.andreani@psi.ch; urs.baltensperger@psi.ch; josef.dommen@psi.ch; johannes.keller@psi.ch; andre.prevot@psi.ch)

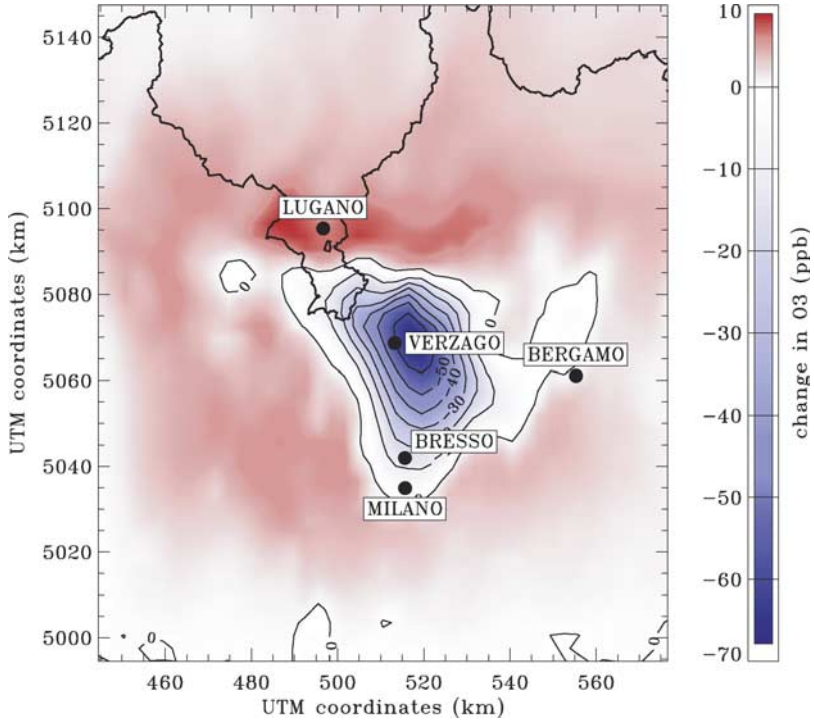

Figure 8. Changes in predicted O_3 mixing ratios (ppb) due to a 35% reduction of anthropogenic NO_x and VOC emissions on 13 May, 1500 CEST. Blue indicates volatile organic carbon (VOC) sensitive and red NO_x sensitive areas.

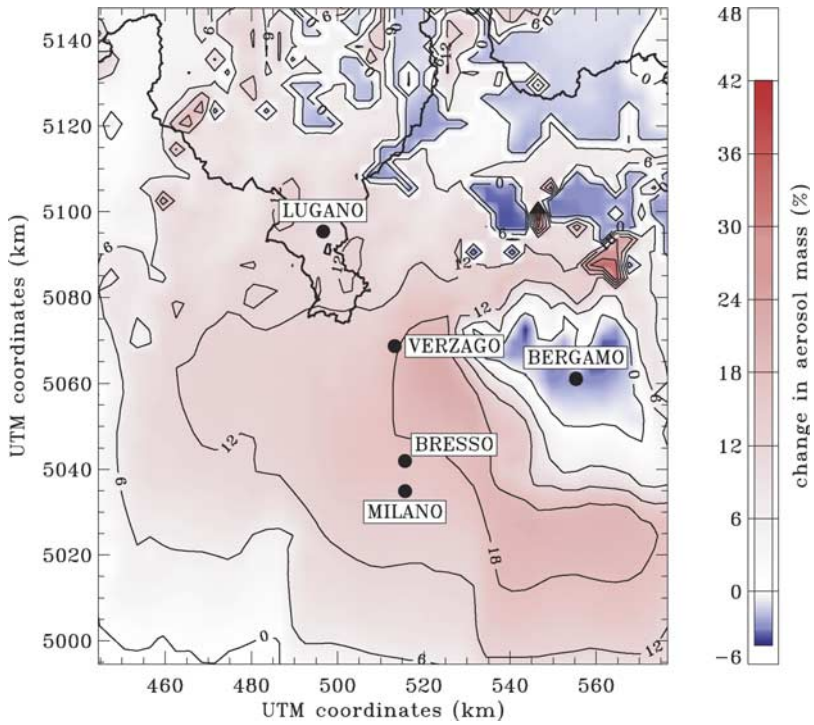

Figure 10. Changes in predicted secondary aerosol mass concentration (%) due to a 35% reduction of NO_x and NH_3 emissions on 13 May, 1500 CEST. Blue indicates NO_x sensitive and red indicates NH_3 sensitive areas.